

# We are IntechOpen, the world's leading publisher of Open Access books Built by scientists, for scientists

6,900

Open access books available

186,000

International authors and editors

200M

Downloads

Our authors are among the

154

Countries delivered to

TOP 1%

most cited scientists

12.2%

Contributors from top 500 universities



WEB OF SCIENCE™

Selection of our books indexed in the Book Citation Index  
in Web of Science™ Core Collection (BKCI)

Interested in publishing with us?  
Contact [book.department@intechopen.com](mailto:book.department@intechopen.com)

Numbers displayed above are based on latest data collected.  
For more information visit [www.intechopen.com](http://www.intechopen.com)



# Fourier Transform Infrared Spectroscopy in the Study of Hydrated Biological Macromolecules

Maria Grazia Bridelli

Additional information is available at the end of the chapter

<http://dx.doi.org/10.5772/66576>

## Abstract

The interaction between biological macromolecules (proteins, nucleic acids, lipids and other biomolecules in the cell) and environmental water is an important determining factor in their conformational properties, stability and function. The hydration processes of biopolymers have been extensively studied in the past 20 years with reference to a considerable variety of models and concepts. In all recent works, a distinction is made between intracellular water that maintains the ordinary liquid state (bulk water) and water ordered in extended hydrogen-bonded lattices at the surface and structured in the internal grooves of macromolecules (hydration water) in dependence on the chemical properties of the macromolecule surface. FTIR spectroscopy has been implemented in this field both for the sensitivity in the conformational analysis of biological macromolecules and the reliability in the investigation of the water network. A perturbation technique such as dehydration-rehydration treatment modifies the macromolecule structure and water distribution. It was applied to two structurally different proteins: lysozyme, a globular ( $\alpha + \beta$ ) protein and collagen, a fibrous protein characterized by the triple helix structure. Submitted to the treatment both of them display irreversible conformational changes.

**Keywords:** FTIR spectroscopy, biological macromolecules, hydration, adsorption isotherms, lysozyme, collagen

## 1. Introduction

Water controls and affects in large extent structure and function of biological macromolecules [1]. This unique molecule has had an essential role in the evolution of living systems, and its functions are manifold. At macromolecular level, very small water amount or small aggregates are fundamental both in the determination and maintenance of the biologically active

structure of proteins, nucleotides, carbohydrates and other biopolymers. The solvent organization around the solute macromolecule structures allows folding to the native and functional conformation and the development of many biological functions such as for example, substrate recognition and binding to an enzyme, protein subunits assembling and to originate and stabilize higher order structures such as membranes. A lot of biochemical reactions fundamental in metabolism and synthesis are involving water as universal reagent, such as hydrolysis, condensation, reduction and oxidation. Despite the great interest in the problem, the relationship between the biopolymer conformation and the structure of the water network cannot still be described with confidence. In the case of proteins, it is well-known that polypeptide molecules are surrounded in the cell by a hydration shell which can be described as formed by differently interacting water molecules organized in layers surrounding macromolecule. The simplified description of the hydration shells formed by a uniform layering of water molecules around the macromolecule is not realistic: most proteins, for example, offer a surface where binding sites, cleft or crevices provide favorable environments for solvent molecules. Such water molecules are organized in clusters or patches decorating the macromolecule surface and are called "bound" water due to the restricted mobility with respect to the water molecules in bulk. Orientation changes may be related to structural or conformational differences among macromolecules. The bond strength variety of bound water affects mobility, reorientation and vibrational properties [2–7].

A variety of experimental techniques were introduced and applied to study the hydration properties of biological macromolecules: DSC (differential scanning calorimetry), NMR (nuclear magnetic resonance), neutron and X-ray diffraction, gravimetric techniques, as well as UV-vis and CD spectroscopies have been employed to characterize the extent of water-biomolecules interaction. In addition, the problem of water interactions was object of theoretical analysis and structure prediction as well as molecular dynamics simulations.

Fourier transform IR absorption spectroscopy represents a powerful method to gain structural information on hydrated biological macromolecules, alternative to other well-established techniques whose application presents severe limitation to dry compounds or in the first hydration events. It requires a minimal sample amount and preparation, and it can be used in a wide variety of conditions and geometries. It enables to study (1) the amplitude and position changes of the main absorption bands associated with characteristic functional macromolecule groups, as a function of water content; (2) the properties of water structured around the biomolecules, using  $\text{H}_2\text{O}$  molecules as probes to detect conformational changes in the macromolecule structure induced by water interactions [8].

$\text{H}_2\text{O}$  displays a strong IR spectrum with three main bands corresponding to the OH stretching, bending and libration modes. Their contribution can be identified in the spectrum of macromolecules and changes in the hydration conditions significantly influence the infrared spectral pattern. The spectral changes observed as a function of water removal may be monitored, correlated to the changes in macromolecule conformation and used to identify the sites of water sorption. The OH stretching band, in particular, by appropriate mathematic manipulation, can be used to build the water adsorption-desorption isotherms describing the hydration processes governing each water population.

The technique and the related experimental procedures were successfully applied in the past on two macromolecular systems very different in chemical composition and structure. Melanin and lipid array have been object of past publications [9, 10]. The present work is concerning two proteins, collagen and lysozyme, and their interaction with water.

## 2. Infrared spectroscopy of water

Water has a strong absorbance in the infrared [11–13]. The characteristic normal modes of the H<sub>2</sub>O molecule are due to vibrating O–H bond whose frequencies are critically dependent on the aggregation state of water: gas, liquid and solid. In the medium infrared wave number region (MIR), the isolated water molecule (gas phase) has three main normal modes of vibration. The symmetric and asymmetric OH stretching vibrations ( $\nu_1$ ,  $\nu_3$ ) have band maximum at 3656 and 3755 cm<sup>-1</sup> and the bending mode,  $\delta(\text{OH})$ , has the band center at 1594 cm<sup>-1</sup>. Upon formation of hydrogen bonds in the liquid phase and because of the broadening of the spectral features,  $\nu_1$  and  $\nu_3$  features are collapsing to a diffuse absorption band that appears 200–400 cm<sup>-1</sup> shifted towards high wave number region with respect to the gas phase values. In addition,  $\nu(\text{OH})$  band width at half-maximum (FWHM) will broaden as a consequence of the H bond pattern formation. In general, the more heterogeneous are the molecular environments of hydrogen-bonded molecules, the broader the band. For this reason, the liquid water spectrum is broader than that found for ice spectrum reflecting the vibrations of more selected hydrogen bond energies and configurations. The bending mode shifts towards high wave number region as a consequence of formation of hydrogen bonds: liquid water and ice display bending absorption bands at 1645 and 1670 cm<sup>-1</sup>, respectively. Libration modes  $\nu_L$  are other vibrational modes of condensed phase water. They appear at 685 cm<sup>-1</sup> for liquid water and shifts at 830 cm<sup>-1</sup> for ice. Moreover, an absorption band is observed around 2200 cm<sup>-1</sup>, centered at 2100 cm<sup>-1</sup> for liquid water and around 2255 cm<sup>-1</sup> for different phases of ice. It represents a combination band, due to the association of the bending  $\delta$  and libration  $\nu_L$  features.

### 2.1. OH stretching band ( $\nu(\text{OH})$ )

The IR OH stretching band has been widely studied to investigate the properties of water structured around biomolecules. The first pioneering work concerning the study of hydration water of globular proteins was performed by Buontempo, Careri and Fasella in 1972 by analyzing the differential Infrared band near 3300 cm<sup>-1</sup> in the spectrum of Lysozyme and Bovine Serum Albumin before and after dehydration under various conditions [14]. The study evidenced the presence of water molecules differently mutually interacting and with the protein surface, being possible to distinguish a contribution due to liquid water and a component corresponding to the so-called tightly bound water. In the following years, thanks to the implementation of the interferometric spectrophotometers instead of the dispersive one, measurements were performed with a much better sensitivity and reliability. The enhancement in the peak fitting procedures with help of second derivative operation and iteration procedures allowed to improve the qualitative picture by fitting the band into component sub-bands

related to different local H bonding structure. In the paper of Onori and Santucci [15] and Mallamace et al. [16], the best fit deconvolution of the band was performed in the study of, respectively, AOT hydrated micelles and lysozyme at different temperatures to investigate structural dynamical transitions.

Pure water  $\nu(\text{OH})$  band ( $3800\text{--}2800\text{ cm}^{-1}$ ) cannot be fitted by a single Gaussian line, but can be deconvoluted into components, usually assigned to different sets of molecules. Following the central limit theorem stating that the distribution of the sum (or average) of a large number of independent, identically distributed variables will be approximately normal, regardless of the underlying distribution, the component number could be enormously large. However, the structural constraints settled on the basis of the number and strength of hydrogen bonds in different arrangements avoids effects of overfitting, allowing the breakdown of the band up to a maximum of six sub-bands in dependence on the model assumed to describe water system. The structure of  $\nu(\text{OH})$  band is described in details by Schmidt and Miki [17] and directly related to the O-H bond lengths: variations in the bond lengths are caused by the influence of the surrounding hydrogen-bonded network of water molecules and affect position and width of the components bands. According to this view, from the higher wave number region towards the lower one, the first peak ( $3680\text{ cm}^{-1}$ ) can be attributed to monomer-like vibration, due to free O-H vibration of  $\text{H}_2\text{O}$  molecules behaving as in the vapor state. The three intermediate components contribute 85% to the total signal, indicating that the majority of water molecules have a local hydrogen-bonded network which includes 3–7  $\text{H}_2\text{O}$  molecules as confirmed by theoretical calculations. Solid clusters (6–10  $\text{H}_2\text{O}$ ) is responsible for the envelope of the two low wave number bands. The peak position of each band was related to O-H bond length. The values were calculated by transforming the frequency and full-width half-maximum values of the  $\nu(\text{OH})$  band components using Badger's rule [18].

In recent times, we have developed a technique operating the removal from the spectrum of the features due to the spurious vibrational bands unrelated to water by means of the operation of subtraction of the “dry sample” spectrum, i.e., the spectrum of the sample gently dehydrated to expel as much solvent as possible without affecting the molecule structure [9, 10, 19]. The cleaned band obtained by such procedure can be treated as a water  $\nu(\text{OH})$  band and therefore compared with the corresponding band of pure water and analyzed by deconvolution in component bands, each one related to different hydrogen bond engagements and lengths.

### 3. Experimental section

Infrared spectroscopy is an experimental technique able to detect the absorption of infrared radiation by the matter [20]. Characteristic vibrational states may be attained by the molecule at the frequencies characteristic for each component molecular group. They can be measured as an absorption spectrum, i.e., a plot of the absorbed intensity of the applied radiation, expressed as absorbance, as a function of its frequency, measured in terms of wave number ( $\text{cm}^{-1}$ ). The infrared spectrum is characteristic for any molecule to such an extent that it may



be considered the molecule fingerprint. For a molecule that consists of  $N$  atoms, there are  $(3N-6)$  ways in which the molecule can vibrate, or  $(3N-5)$ , if it is linear, therefore, it is reasonable to expect that complex molecules or mixture of substances could originate complex IR spectra, difficult to analyze and to interpret. Nevertheless, some moieties of the molecules, the so-called functional groups, display one or more absorption infrared bands at specific frequencies, slightly influenced by the surrounding parts of the molecule. In such a way, it is possible to identify the chemical groups responsible for such features even though the molecule is not known.

FTIR spectrophotometers use the technique of Michelson interferometry to simultaneously sample a range of frequencies. The IR beam emitted by the source is collected by a beam splitter and divided into two beams each one of half intensity with respect to the original beam. One is falling on the moving mirror and the other one on the fixed mirror. The light beams reflected by the moving and the fixed mirrors are combined generating a complex interferogram, as a function of the position of the moving mirror. The resulting interferogram is subjected to Fourier analysis to generate a spectrum, i.e., a plot of intensity versus frequency. Absorption spectra are obtained by measuring the interferograms with a sample and with the empty sample cell (blank) in the beam, being the interferogram intensity

$$I_{\text{interferogram}}(t) = k \int_{-\infty}^{+\infty} I_{\text{beam}}(\nu) e^{i2\pi\nu t} d\nu \quad (1)$$

where  $k$  is a constant,  $I_{\text{beam}}$  the intensity of the beams and  $\nu$  the wave number. From the interferogram, the intensity of the beams can be calculated by inverse Fourier transforming the resulting interferograms

$$I_{\text{beam}}(\nu) = k \int_{-\infty}^{+\infty} I_{\text{int}}(t) e^{-i2\pi\nu t} dt \quad (2)$$

The IR absorption spectrum is calculated as the logarithm of the intensity quotient of blank to sample.

### 3.1. Equipment and materials

Any standard commercial Fourier transform infrared spectrophotometer can be used to perform the experiments described in the present paper. We have used two kinds of equipment: BOMEM DA8 and Jasco 420 FTIR spectrophotometers operating in the  $4000\text{--}400\text{ cm}^{-1}$  range, at temperature close to ambient ( $290\text{--}300\text{ K}$ ). Each spectrum was measured by acquiring 128 scans at  $2\text{ cm}^{-1}$  spectral resolution.

The samples were thin films obtained by depositing aqueous solutions ( $c = 10\text{--}40\text{ mg/ml}$ ) on  $\text{CaF}_2$  windows and allowing them to dry in air under ambient conditions. The film smeared on the calcium fluoride platelets was assembled in a sealed sample cell consisting in a dry box equipped with IR transparent  $\text{CaF}_2$  windows. In the box were inserted (1) a vessel containing a saturated salt solution suitable to assess the opportune relative humidity (RH) to which the sample has to be equilibrated; (2) the sample prepared as a film smeared on a  $\text{CaF}_2$  platelet, vertically positioned in such a way as to allow for transmission measurements (**Figure 1**). The box, avoiding any contact of the sample with the external atmosphere, was inserted in the sample chamber of the FTIR spectrophotometer.

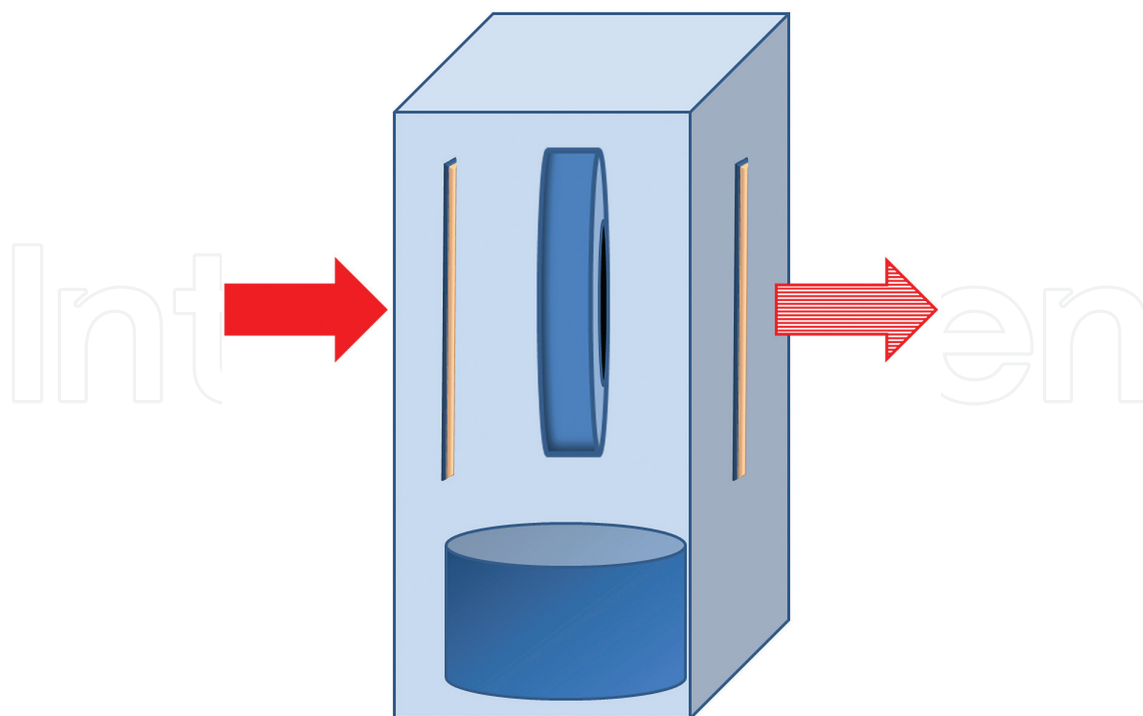


**Figure 1.** Sketch of the sample holder employed to attain the desired hydration degree in the samples. The samples were obtained as films of macromolecule solution smeared on the vertical  $\text{CaF}_2$  platelet, allowed to dry in air before to expose them to the moist ambient in the box. Different relative humidity was achieved in the inner ambient of the box by saturated salt solutions put in the vessel placed on the box base and assembled together with the sample.

Blank measurements were recorded on the sample holder in order to subtract the contribution of the  $\text{CaF}_2$  platelet on which the sample was deposited and the spectrum of the dry box  $\text{CaF}_2$  windows.

### 3.2. Experimental procedures and analysis of water sorption

The protein film together with the salt solution suitable to keep it at the desired humidity level was assembled in the sample holder for 1–2 days before to submit it to the measurements. **Table 1** lists the salts employed for preparing salt solutions able to provide in the desiccator water activities  $a_w$  ranging between 0.06 and 0.97.

The change in the hydrating solution was performed in a dry box under a controlled  $\text{N}_2$  atmosphere. The lowest hydration value was reached by maintaining the sample in an oven at about  $80^\circ\text{C}$  for 2 h. This sample was called the “dry” sample.

Fitting operation of the OH stretching and Amide bands was performed according to Gaussian curves starting from a second derivative analysis [21]. In particular, the OH-stretching mode band ( $\nu \sim 3400 \text{ cm}^{-1}$ ) was analyzed following the approach, adopted in the literature to describe the solvent role of water and deconvoluted into components, which, in principle, might be related to different hydrogen-bond distances [17]. A twofold analysis was performed on the  $\nu(\text{OH})$  band. First, the spectra of the samples collected by decreasing (desorption run) and increasing (adsorption run) the ambient relative humidity were compared and analyzed with

Salt	$a_w$
NaOH	0.06
KOH	0.09
CaBr <sub>2</sub>	0.16
CaCl <sub>2</sub>	0.29
NaI	0.38
Ca(NO <sub>3</sub> ) <sub>2</sub>	0.51
NaBr	0.58
KI	0.69
NaNO <sub>3</sub>	0.74
NaCl	0.75
NH <sub>4</sub> Cl	0.79
KBr	0.81
KCl	0.84
BaCl <sub>2</sub>	0.90
KNO <sub>3</sub>	0.92
K <sub>2</sub> SO <sub>4</sub>	0.97

**Table 1.** Salts employed for saturated salt solutions necessary to accomplish the controlled activities  $a_w$  in the box where the macromolecule films were equilibrated before FTIR measurements.

respect to the other spectral features (Amide bands). Second, the OH stretching band was resolved, by a curve fitting approach, in Gaussian components. The goal in the method is to decompose the feature into three component bands which can be assigned to three different sets of hydrogen bond strength. The Gaussian component amplitude, converted into water amounts, can be used to plot sorption isotherm curves [22]. The relative amounts of water in the three different structural forms were expressed in terms of the area of each peak by assuming that the sum of the areas of the peaks is proportional to the total amount of water in the protein. The corresponding H bond lengths were evaluated by employing Nakamoto plots [23].

Water sorption isotherms were obtained as the sorbed water vapor amount versus water vapor activity  $a_w$  at fixed temperature [22]. The water content of the sample was spectrophotometrically determined from the  $\nu(\text{OH})$  band amplitude subtraction of the spectrum of the same sample fully dehydrated (“dry” sample). In this way, any contribution to the band of N–H and C–H stretching vibrations, occurring in the same wave number range, was systematically eliminated. Due to the thin thickness of the samples, layered as film and the very low water content ( $0.97\text{--}0.06\text{ g}_{\text{water}}/\text{g}_{\text{dry sample}}$ ), the very small change in the optical path produced by dehydrating the sample does not affect significantly the spectra intensity. Adaptation of Beer's law was successively used to rescale the intensity of the “cleaned”  $\nu(\text{OH})$  bands, in



accordance with the approach proposed in the literature to study various hydrated biomaterials [24]. To quantify the integrated absorbance in terms of water surface coverage, we can assume a modified form of Beer-Lambert' law

$$\tilde{A} = \int_{band} A d\nu = \varepsilon(\nu_{MAX}) \bar{c} d \quad (3)$$

where  $\tilde{A}$  is the integrated absorbance of the component band,  $\varepsilon(\nu_{MAX})$  is the molar absorptivity at wave number  $\nu_{MAX}$  corresponding to the peak of the band ( $\text{L mol}^{-1} \text{cm}^{-1}$ ),  $\bar{c}$  is the concentration of the absorbing species ( $\text{mmol/cm}^3$  or, equivalent  $\text{mol/L}$ ) and  $d$  is the average thickness of the absorbing species film, that is, adsorbed water, in centimeters [9].

For water, it is possible to evaluate the molar absorptivity  $\varepsilon(\nu)$  at fixed wave number [24]: for example, one can evaluate  $\varepsilon(3600 \text{ cm}^{-1}) = 1.647 \text{ L mol}^{-1} \text{cm}^{-1}$ . By assuming the path length  $d$  as the thickness of a film of water, the corresponding amount of the water content can be converted in concentration  $\bar{c}$  of water, assumed as only absorbing species. The concentration  $\bar{c}$  in each sample prepared at each hydration degree can be evaluated and employed to normalize the amplitude of the subcomponents in the  $\nu(\text{OH})$  band. The desorption-adsorption branches of the isotherm curves were therefore obtained for each Gaussian component. As a rule, the desorption experiments were performed by starting from the highest  $a_w$  value ( $a_w = 0.97$ ) and accomplished before the adsorption one, to avoid possible damages in the samples produced by dehydration treatments.

## 4. Collagen

Collagens are a large protein family forming a characteristic triple helix of three polypeptide chains giving rise to supramolecular structures in the extracellular matrix: their size, function and tissue distribution vary considerably [25]. So far, 26 genetically distinct collagen types have been described. It is the main fibrous component of skin, bone, tendon and cartilage, accounting in particular for three-quarters of the dry weight of skin, and representing the most prevalent component of the extracellular matrix. The collagen molecule is a rigid rod-like structure able to resist stretching. It is composed of three polypeptide left-handed  $\alpha$  chains coiled around each other to form a typical right-handed rope-like triple helical rod (approximately, 1.5 nm in diameter, 300 nm in length). The triple helical sequences are composed of Gly-X-Y repeats, X and Y being frequently proline and hydroxy-proline, respectively [26]. Stabilization of the triple helix is assured by a lot of structural conditions as the presence of glycine as every third residue, a high content of imino acids with a rigid cyclical structure (proline and hydroxy-proline) and electrostatic interactions involving lysine and aspartate [27]. Both in the structural and functional properties, a key role is undoubtedly played by water, which provides inter-chain hydrogen bonds and water bridges and coats triple helix by a cylinder-like of hydration [28, 29]. Moreover, water critically regulates chain flexibility and assures the water mediated H-bonds favoring fiber recognition and alignment. Water lacking is a very dangerous process for the protein, damaging the structure in irreversible way. Water depletion, caused by tissue maturation, exposition to UV light and/or some pathological processes, such as diabetes, triggers detrimental conformational rearrangements

due by nonenzymatic glycation reactions between the protein and the complex carbohydrates present in the matrix, leading to the formation of oxidation products, known as Advanced Glycation End-products (AGE) [30, 31] having the effect to modify the collagen fibers physical properties, inducing an increase in stiffness and breaking load, denaturation temperature, solubility and a decrease in resistance to degradative enzymes [32].

Despite the great amount of studies [33], the explicit relationship between protein and hydration water structure is still an open question and the detailed dehydration scheme of collagen and the structural implications are not yet completely elucidated.

#### 4.1. Hydration structure of collagen: FTIR spectroscopy and water sorption isotherms

Complementary FTIR measurements on collagen prepared at very low hydration level ( $a_w$  in the range 0.06–0.97) and adsorption isotherm technique have put in evidence the critical hydration level which induces an irreversible conformational change in the protein, responsible for the first ageing step.

In **Figure 2**, the spectra of collagen extracted from rat tail tendon (type I collagen) are shown during the dehydration run.

In order to study the role of water interacting with collagen, FTIR spectrum was analyzed in the OH stretching region by changing the hydration content of the sample following the method described above (Section 3.2).

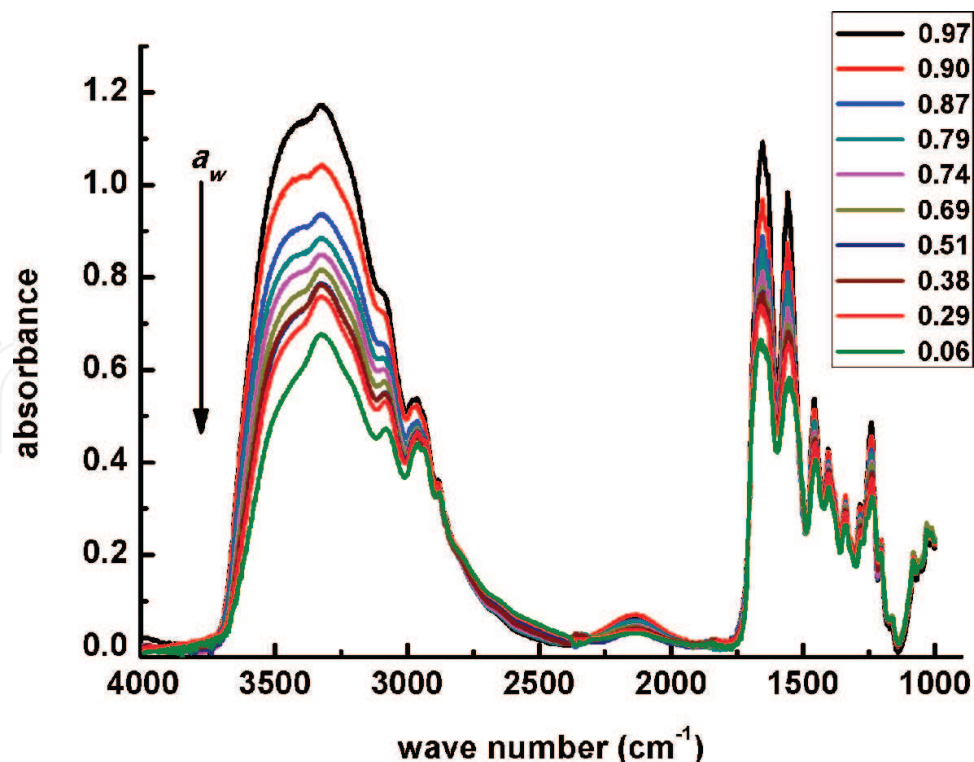


**Figure 2.** FTIR spectra of rat tail tendon collagen, recorded at different water activities during dehydration treatment from  $a_w = 0.97$  to  $a_w = 0.06$ .

OH stretching band (wave number range 4000–3000  $\text{cm}^{-1}$ ) was analyzed after subtraction of the “dry” spectrum and decomposed into four components (**Figure 3**) whose frequencies were related to different O-H bond lengths as listed in **Table 2**.

The  $\nu(\text{OH})$  feature composition in Gaussian sub-bands in such a way can be correlated to the hydrogen bond network around the protein and provides information about the structural modifications induced by changing the hydration level. The four Gaussian components are peaking, for the sample at the maximum hydration, at 3598, 3467, 3295 and 3115  $\text{cm}^{-1}$ , following the procedure of the second derivative analysis. They are corresponding to four classes of water molecules bound to the protein, different in vibrational energies and each one characterized by a single average H-bond distance ( $\text{H}\cdots\text{OH}$  length): 0.31, 0.29, 0.28 and 0.25 nm, respectively [18, 23].

The sub-band peaking at the highest wave number region is corresponding to H-bond distances characteristic of vapor-like state. Similar features, detected for different biological macromolecules [9, 10, 16], were assigned to the non-H-bonded or weakly H-bonded O-H groups. It is reasonable to suppose that in collagen prepared at very low hydration levels, as in our case, they could be originated by the dangling most external water molecules sitting on the outer hydration layer coating the macromolecule. The inability for these molecules to establish active H-bonds with surrounding water molecules, accounts for the high mobility and the large vibrational energy comparable with those of free water molecules in the vapor state. They represent about the 5% of the total amount of water hydrating collagen at the relative humidity settled for the experiment, being the percentages calculated as the

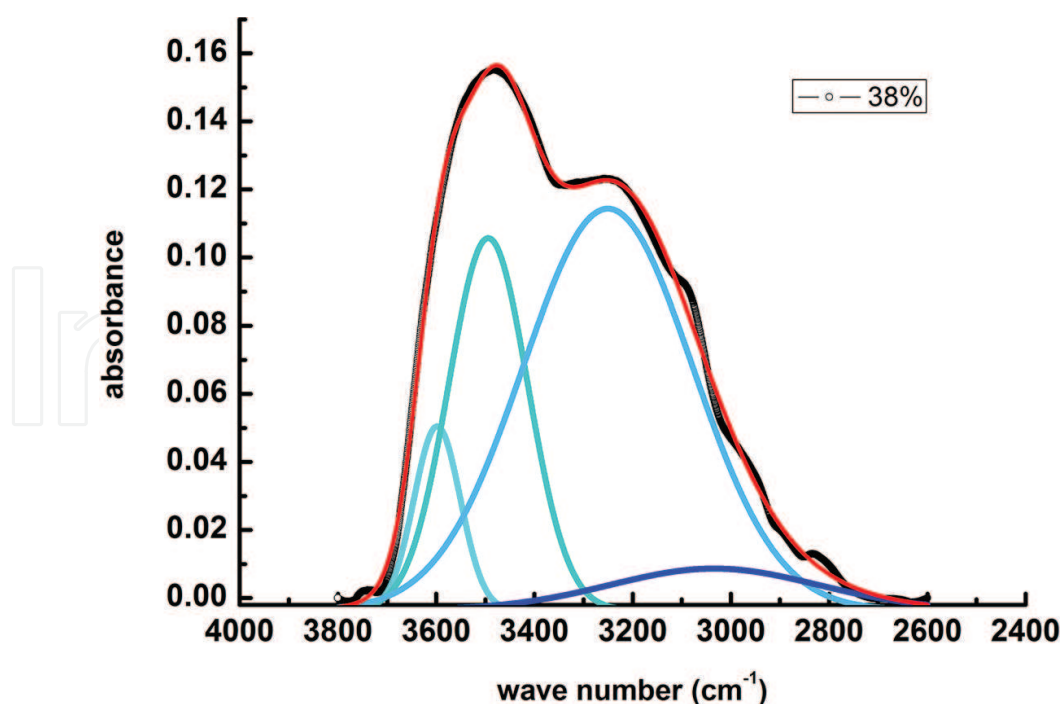


**Figure 3.** Gaussian deconvolution of FTIR spectrum of collagen ( $a_w = 0.38$ ) in the  $\nu(\text{OH})$  region, by means of four component bands, as obtained by means of second derivative method. The sum of the fitted curves is shown as the red line, closely overlapping the experimental data trace, which is shown as a full black line.

Molecule	Stretching frequency (cm <sup>-1</sup> )				H-bond distances (nm)			
	$\nu_1$	$\nu_2$	$\nu_3$	$\nu_4$	$d_1$	$d_2$	$d_3$	$d_4$
Pure water	3570	3434	3322		0.30	0.29	0.28	
Collagen	3598	3467	3295	3115	0.31	0.29	0.28	0.25
Lysozyme	3539	3315	3008		0.29	0.28	0.24	

**Table 2.** Hydrogen bond distances estimated from the vibrational frequencies following Nakamoto et al. [23].

ratio  $A_i/A_{\text{tot}}$  of the single component area ( $A_i$ ) with respect to the total band area ( $A_{\text{tot}}$ ). The two component bands peaking at the intermediate wave numbers may be related to H<sub>2</sub>O molecules coordinated by two or three, more or less distorted or strained, H bonds. They may be identified with H<sub>2</sub>O molecules deeply located inside the protein helix, acting as water bridges within a single peptide chain and/or interconnecting the different  $\alpha$ -chains in the triple helix. They constitute the 19% and the 31%, respectively, of the total water amount. The corresponding H-bond distances suggest that they could represent the solvation molecules involving C=O groups belonging to glycine ( $d(\text{C}=\text{O}\cdots\text{W}) = 0.295$  nm) and hydroxyproline (Hyp) ( $d(\text{C}=\text{O}\cdots\text{W}) = 0.284$  nm) hydroxyl moieties [29]. The component at 3180 cm<sup>-1</sup> may be attributed to water molecules located near to the protein surface and hydrogen bonded to polar and charged groups exposed to the macromolecule surface: they originate some ice-like tetrahedral structures more or less distorted. The corresponding average H bond length is in fact characteristic for arrangement of H<sub>2</sub>O molecules as in small solid water clusters, assuming the length O $\cdots$ O of hydrogen bonds in ice as 0.276 nm [34]. The broad profile of such a band, extending on a wide wave number range, testifies for the large distribution of water vibrational states in a configuration variety, concurring to the feature. Such a sub-band represents the main hydration fraction at the highest settled humidity, corresponding to the 45% of the total amount of hydration water.

The dehydration treatment at  $a_w = 0.06$  followed by a subsequent rehydration up to the original relative humidity ( $a_w = 0.92$ ) reveals a pronounced hysteresis effect in the  $\nu(\text{OH})$  band amplitude and a remarkable modification of the profile, as shown in **Figure 4**.

The difference spectrum is peaking at  $\nu \sim 3400$  cm<sup>-1</sup>; therefore, it is roughly filling the position of the third component of the overall  $\nu(\text{OH})$  band. Moreover, it exhibits a shoulder on the low wave number side ( $\nu \sim 3000$  cm<sup>-1</sup>). This finding suggests that dehydration treatment causes in collagen the loss of a considerable amount of H<sub>2</sub>O molecules truly involved in the internal water bridges, probably coordinated by glycine C=O, and a fraction of molecules coating the polypeptide surface, bound to the Hyp hydroxyls. This water portion once desorbed, only partially can be re-adsorbed. It accounts for the 21% of the total water amount initially hydrating the sample.

With the aim to better investigate this topic, the peak areas of the two intermediate sub-bands, peaking at  $\nu = 3467$  cm<sup>-1</sup> and  $\nu = 3295$  cm<sup>-1</sup>, detected in the spectrum of the sample at the highest hydration level, were plotted as a function of the activity  $a_w$  during the desorption and the subsequent adsorption processes to build the corresponding isotherm curves. **Figure 5** summarizes the isotherm curves related to the two component bands highlighting the large differences occurring in sorption mechanisms of the two related water sets.

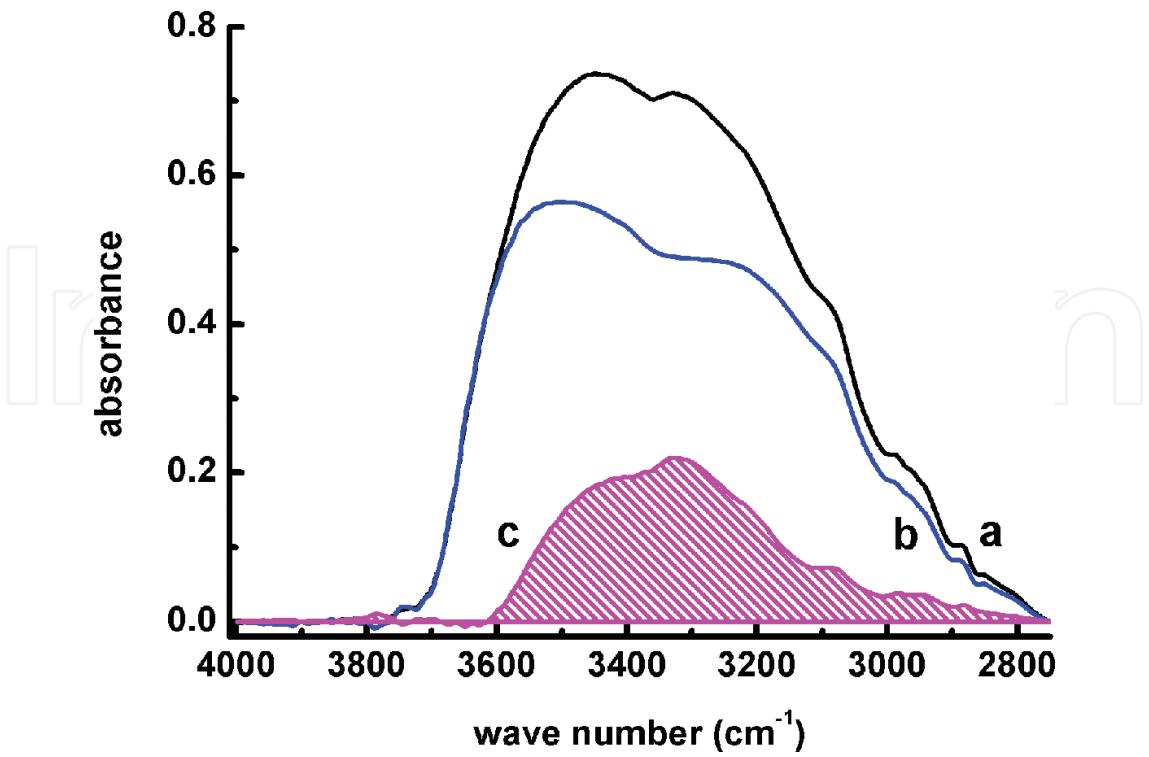


**Figure 4.** OH stretching bands measured for collagen at  $a_w=0.97$ , before (curve a) and after (curve b) dehydration at  $a_w=0.06$ . Curve c represents the difference between a and b bands and the subtended area (pink dashed area) can be related to the water amount desorbed by the sample during dehydration and no more recovered along rehydration.

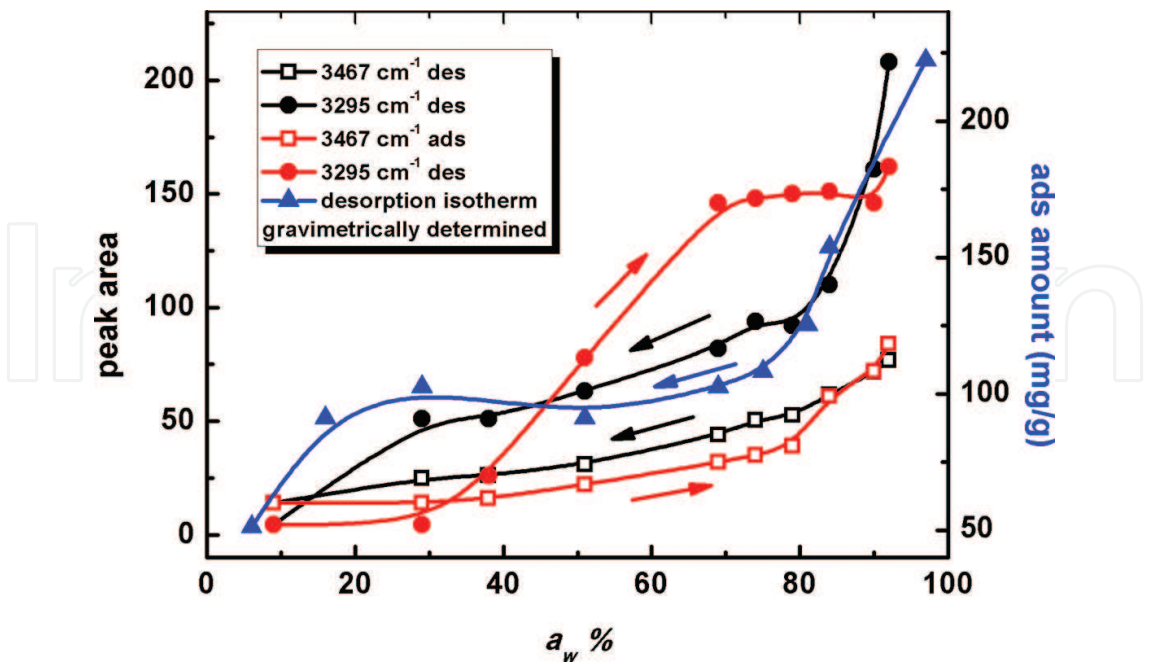


**Figure 5.** Desorption and adsorption curves for two sub-bands ( $\nu=3467\text{ cm}^{-1}$  and  $\nu=3295\text{ cm}^{-1}$ ) of OH stretching band measured for collagen, during dehydration (black symbols) and re-hydration (red symbols) treatments. Blue triangles represent the desorption data obtained by means of the gravimetric experiment. The lines are a guide for the eye.



The band at  $3295\text{ cm}^{-1}$  displays a type II-like desorption and adsorption behavior [22]. The band amplitude completely recovers at the end of the process; therefore, such component only partially participates to the lacking of recover in amplitude of the total  $\nu(\text{OH})$  band, the weak hysteresis effect being probably due to the reassessment of the interchain water bridges as a consequence of the perturbation induced by water subtraction. Concerning the band at  $3467\text{ cm}^{-1}$ , the mechanism of dehydration is very different than that of rehydration. The desorption branch correlates well with the curve gravimetrically measured by weighing the sample after equilibration at each different humidity level, as shown in **Figure 5** (blue full triangles): the two desorption curves show the same trend. They are as type II curve, where three phases can be distinguished: a starting rapid dehydration step from  $a_w = 0.92$  to about  $a_w = 0.80$ , a second one in the  $a_w$  range  $0.80\text{--}0.40$ , where water desorption occurs more slowly with the decrease in ambient relative humidity and a third phase at low water activities, extending from  $a_w = 0.40$  to  $a_w = 0.06$ , describing a characteristic “knee” [2]. The first phase may be assigned to the removal of water molecules forming hydrogen-bonded clusters, the second one to subtraction of  $\text{H}_2\text{O}$  molecules from weakly interacting surface regions and the third branch to the dehydration of strongly bound water molecules by Hyp hydroxyl moieties exposed at the surface. The result suggests that the whole protein desorption process is mainly concerning the dehydration of the external water layer.

Water uptake exhibits a very different behavior with respect to the dehydration, resulting in a large hysteresis loop, extending over the whole activity range. Adsorption isotherm displays features not conform to any isotherm type in the Brunauer classification [22]. From  $a_w = 0.06$  to  $a_w = 0.40$ , the amount of water adsorbed is rather negligible. The activity  $a_w = 0.40$  represents a threshold activity above which a sudden water uptake occurs attaining a saturation hydration value, lower than the moisture content of the freshly prepared sample.

Water deprivation and restitution has considerable consequences on the macromolecule structure. The changes in the high wave number region of the IR spectrum can be correlated with the secondary structure analysis carried out on Amide I band which was resolved in Gaussian components. Qualitative and quantitative information about the conformational composition of the protein prepared in the different hydration states were obtained. Amide I band in fact was decomposed in sub-bands whose position and area were related, respectively, to the different types and to the amount of secondary structures (**Figure 6**). The sum of the areas of the peaks represents the total amount of secondary structure in the protein.

The curve fitting procedure [8, 21] allowed determining the secondary structure composition in the freshly prepared sample ( $a_w = 0.97$ ), as displayed in **Figure 6A**:  $\beta$ -turn ( $1695\text{ cm}^{-1}$ ),  $\beta$ -sheet ( $1680\text{ cm}^{-1}$ ),  $\alpha$ -like helix ( $1660\text{ cm}^{-1}$ ), unordered structure ( $1644\text{ cm}^{-1}$ ), triple helix ( $1628\text{ cm}^{-1}$ ),  $\beta$ -sheet ( $1615\text{ cm}^{-1}$ ), side chains ( $1607\text{ cm}^{-1}$ ). The multipeak decomposition of the band measured in the sample rehydrated at the original activity, after dehydration at  $a_w = 0.06$  (**Figure 6B**), revealed the modification occurred in the secondary structure, the most significant change concerning the increase in the broad sub-band peaking at  $\nu \sim 1670\text{ cm}^{-1}$  largely spanning the high wave number region of the Amide I band and the parallel decrease in the component bands at  $1695$  and  $1660\text{ cm}^{-1}$ . The formation of such structures may be related to the relative increase in  $\beta$  components (antiparallel  $\beta$ -sheet and aggregated strands) with



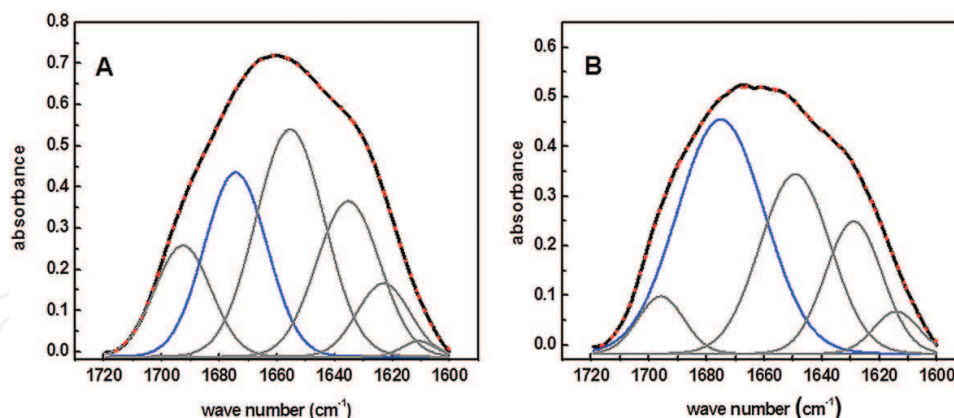


**Figure 6.** Amide I band deconvolution for collagen at  $a_w = 0.97$  before (A) and after (B) dehydration at  $a_w = 0.06$ . The set of Gaussian components can be related to the secondary structure composition of the protein. The full blue lines highlight the component bands related to the antiparallel  $\beta$ -sheet/aggregated strand motif. The dotted red lines represent the sum of the components.

respect to the  $\alpha$ -helix contribution in the Amide I envelope. Such effect may be explained by assuming the formation of bridges among near collagen molecules laterally associating by forming chain structures side by side interacting, involving Hyp residues [35], spectroscopically mimicking  $\beta$ -sheet structures [36].

These results would be consistent with the physiologic behavior of collagen and may be correlated to the changes in the structural properties of collagen fiber assembly as a consequence of dehydration. The spectroscopic data are consistent with specific binding of water molecules to collagen chains stabilizing the collagen triple helix by Hyp residues through intramolecular water bridges. The difference in interfacial surface water may be the physical reason for the hysteresis phenomena observed in water adsorption isotherms. As a consequence of the removal of water down to water activity  $a_w < 0.40$ , the association of the collagen molecules takes place and once water is restituted, the assembled fibers are no more able to re-adsorb all the water available during the rehydration phase. This arrangement, responsible for the lacking in the hydration recover of protein, may be considered one of the main causes of collagen maturation and ageing.

## 5. Lysozyme

Lysozyme is a small globular protein shaped as an approximate ellipsoid of dimension  $45 \times 30 \times 30 \text{ \AA}$  composed of 129 residues, acting as an enzyme causing lysis of Gram positive bacteria by hydrolyzing the  $\beta$ -(1-4) glycosidic links in the cell wall peptidoglycan [37]. Lysozymes have been isolated from a great variety of sources. Lysozyme from hen egg white (HEWL, MW 14600) is an  $\alpha + \beta$  protein with 30% helical residues and 13%  $\beta$ -sheet content. As for the majority of protein molecules, lysozyme structure and stability are largely determined by the interaction between the protein and the aqueous surroundings [38–40]. Investigation of the structural changes occurring during the change in the activity of water was important for understanding the mechanism of this interaction. In particular, Careri et al. [41] suggested a connection between the water-induced onset of enzymatic activity and some water triggered

physical properties of the protein system, i.e., heat capacity, diamagnetic susceptibility, IR absorption, percolation threshold for proton conduction, recognizing that the hydration threshold for lysozyme, occurred at 0.22 g of water/g of protein.

### 5.1. Hydration structure of lysozyme: FTIR spectroscopy and water sorption isotherms

Lysozyme from hen egg white was used without further chemical purification and submitted to FTIR investigation following the experimental method above described (Section 3.2). The solvent architecture around the protein was correlated to the macromolecule conformation by means of two different procedures:

By monitoring secondary structure from the inspection of the changes occurring both in Amide I and Amide III features by changing the protein hydration level. Amide I band analysis in fact suffers from the extensive overlap of the underlying water H–O–H bending band, lying in close proximity ( $\sim 1645\text{ cm}^{-1}$ ), the line broadening making quantitation arduous. The secondary structure assignments can be reinforced by taking into account Amide III, attributed to N–H deformation coupled with the C–N stretching motion and ranging in the wave number region  $1220\text{--}1340\text{ cm}^{-1}$ . It occurs out of any water absorption region and its behavior, monitored along secondary structure changes of the protein, may be correlated with the changes suffered by the enzyme structure to provide a consistent picture of the hydrated protein conformational properties [8].

By studying the evolution of the broad  $\nu(\text{OH})$  feature along the protein hydration and dehydration processes. The OH stretching bands, recorded at each activity value, were decomposed into three Gaussian components, corresponding to the three main water fractions hydrating lysozyme, different in structure and clustering order. By appropriate analysis of the data, sorption isotherm curves were built, able to provide information on relationship between the water content and the different protein structural features. The water amount bound to Lysozyme was deduced from the  $\nu(\text{OH})$  band area after subtraction of the spectrum of the “dry” sample.

**Figure 7A and B** shows  $\nu(\text{OH})$  bands recorded for the protein prepared at different hydration degree along the dehydration and the rehydration runs.

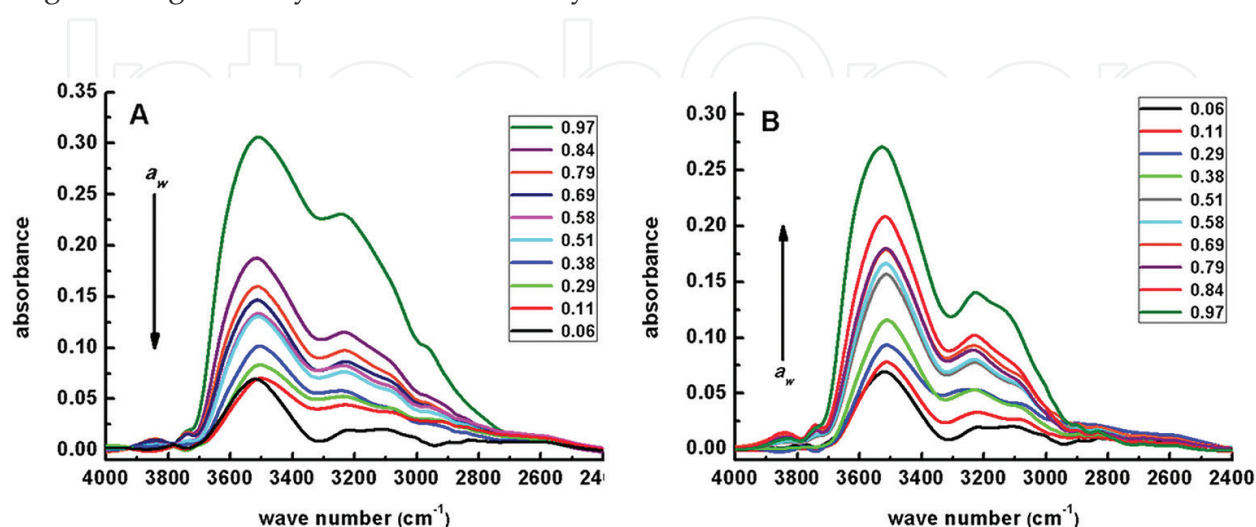


**Figure 7.** OH stretching bands measured for lysozyme along dehydration (A) and rehydration (B) treatments between  $a_w = 0.97$  and  $a_w = 0.06$ .

Following the decomposition of the band in Gaussian components, three sub-bands were detected (**Figure 8**, left side): their positions and the corresponding OH...O distances, measured for the sample at the highest hydration degree, are listed in **Table 2**. First component band (I) (**Figure 8A**) peaking at the higher wave number ( $3539\text{ cm}^{-1}$ ) may be attributed to surface water molecules easily adsorbed on the most external hydration layer. They show the dangling OH vibrational frequency typical for free-like  $\text{H}_2\text{O}$  molecules at the interfaces water-air. The sub-band at  $\nu = 3315\text{ cm}^{-1}$  (II) (**Figure 8B**) may be related to water molecules directly interacting with protein backbone, particularly engaged in hydrogen bonding with peptide carbonyl moieties ( $\text{C}=\text{O}\cdots\text{W}$ ). The broadband at  $\nu = 3008\text{ cm}^{-1}$  (III) (**Figure 8C**), representing the most prevalent component, corresponds to water molecules forming the hydration shells around the protein, interacting with neighboring adsorbed water molecules. The position of the feature is indicative of the intermolecular hydrogen bond distances matching the average

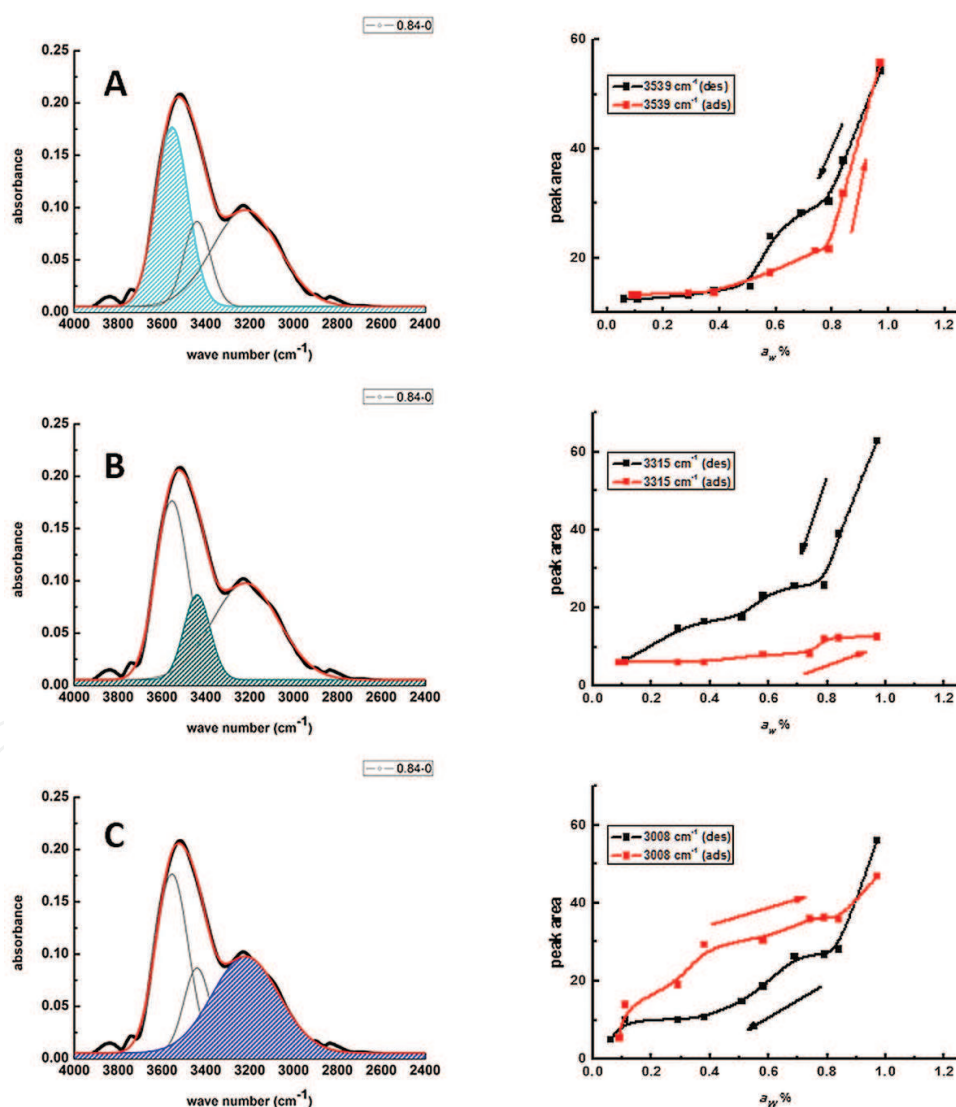


**Figure 8.** Gaussian deconvolution of FTIR spectrum of lysozyme ( $a_w = 0.84$ ) in the  $\nu(\text{OH})$  region, by means of three component bands (dashed areas). For each component band, the isotherm curves were plotted: black symbols represent the desorption data and red symbols represent the adsorption data. The lines are a guide for the eye.

characteristic lengths typical for tetrahedral ice structure but the large bandwidth reveals that it is suffering lengthening and distortions in the distances and orientation.

**Figure 8**, right side, displays the isotherm curves obtained by monitoring the areas of the three component bands as a function of the moisture of the sample, both during the sequential decrease in the water content of the sample and during the opposite treatment, rehydration at RT. Sub-band I gives rise to a desorption isotherm classified as Type IV, characteristic for the evaporation process of water at the interface water-air. In the converse process of condensation, the underlying liquid surface acts as to nucleate the adsorption, therefore, the isotherm is quite different, showing the shape of a Type III curve, characteristic for cooperative interactions. The loop desorption-adsorption gives rise to a hysteresis because evaporation and condensation do not take place as exact reverse of each other. The hysteresis effect indicates that between  $a_w = 0.40$  and  $a_w = 0.80$ , the amount of water desorbed is greater than that adsorbed, suggesting a change or an assessment of the condensation surface, as a consequence of dehydration, until the highest moisture degree is achieved. Sub-band III originates a hysteresis loop as well, although the isotherm curves are not easy to be classified according to the literature [22]. The intermediate component (sub-band II) reveals an anomalous behavior reflecting an irreversible structural modification of the protein. Water desorption describes a Type IV-like isotherm but the adsorption branch is a flat line up to  $a_w = 0.80$ , showing a small increase for the highest hydration values attained, but unable to completely recover the original amplitude. It notifies the inability of the macromolecule to re-adsorb in a reversible manner the water phase originally coordinated by the polypeptide backbone, once desorbed.

The process can be explained by assuming that water subtraction modifies the structural properties of the macromolecule which would tend to narrow down the crevices where water molecules were inserted, by establishing intrachain bonds difficult to reverse. As discussed in the literature, in the absence of water, the protein molecule tends to fill the voids left by water by adopting structures that can continuously fill the space [38]. The hysteresis effect is confirmed by the difference in amplitude between the  $\nu(\text{OH})$  band of the native sample and the rehydrated one after dehydration, as shown in **Figure 9**. The difference band centered at  $\nu \approx 3300 \text{ cm}^{-1}$  corresponds to the water fraction desorbed during the dehydration run and no more re-adsorbed during the subsequent hydration process.

In **Figures 10** and **11**, the spectral windows related to the two polypeptide secondary structures, i.e.,  $1700\text{--}1550 \text{ cm}^{-1}$  and  $1300\text{--}1230 \text{ cm}^{-1}$  corresponding to the Amide I and III ranges are shown for the two samples prepared at the highest hydration degree. The Gaussian decomposition of the native lysozyme Amide I band (**Figure 10**) was carried out in four major components, in agreement with previous studies performed on lysozyme and other kinds of proteins [42, 43]. The band fairly asymmetric and peaking at  $\sim 1656 \text{ cm}^{-1}$ , is mainly due to the contribution of  $\alpha$ -helical structure (75%), in agreement with the literature [44]. The  $\beta$ -sheet content is lower and can be measured from the two components around  $1618$  and  $1684 \text{ cm}^{-1}$ . The component centered at  $1635 \text{ cm}^{-1}$  can be attributed to unordered structures.

**Figure 11** displays Amide III bands for the sample at  $a_w = 0.97$  and after dehydration down to  $a_w = 0.06$ . The curve fitting analysis for lysozyme in the native hydrated form reveals three



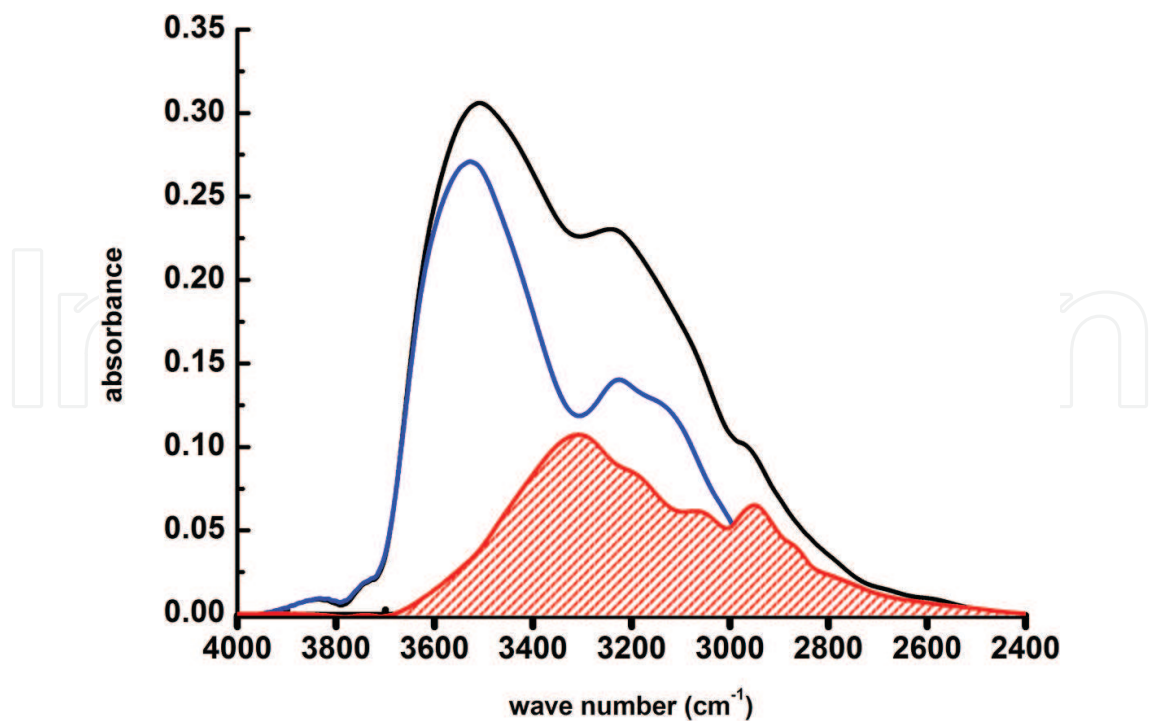


**Figure 9.** OH stretching bands measured for lysozyme at  $a_w = 0.97$ , before (black curve) and after (blue curve) dehydration at  $a_w = 0.06$ . The red curve represents the difference of the two curves and the subtended area (red dashed area) can be related to the water amount desorbed by the sample during dehydration and no more recovered along rehydration.

main sub-bands peaked at 1338, 1320 and 1300  $\text{cm}^{-1}$ , which can be categorized as being  $\alpha$ -helical with a total relative band strength of 40%. The relatively sharp band at 1230  $\text{cm}^{-1}$  is assigned to  $\beta$  sheet structure for 21% and two broadbands at 1260 and 1285  $\text{cm}^{-1}$  indicate the presence of unordered structures for 35%. Dehydration induces modifications of the bands with respect to the spectrum of the native hydrated sample: they can be related to changes in the secondary structure composition.

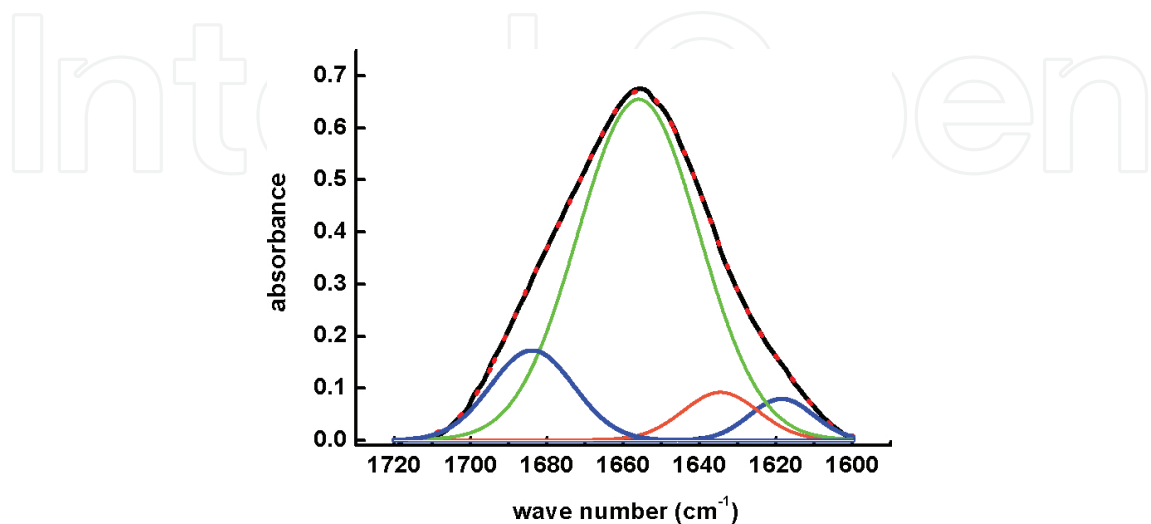


**Figure 10.** Amide I band deconvolution for lysozyme at  $a_w = 0.97$ . The component bands can be related to the structural contribution of  $\alpha$ -helix (green line),  $\beta$ -sheet (blue line) and unordered (orange line) structures.

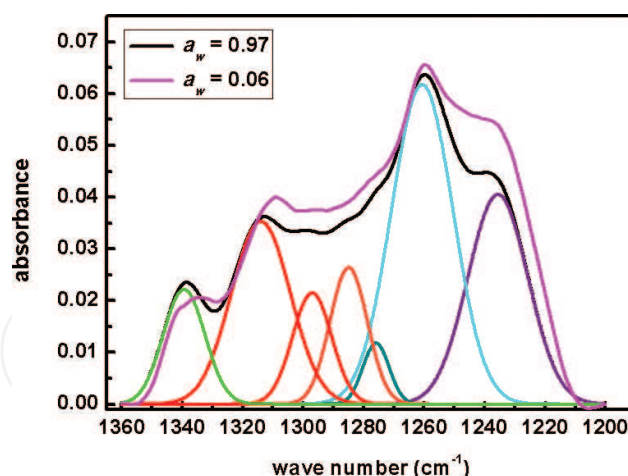


**Figure 11.** Amide III band measured for lysozyme at  $a_w = 0.97$  (black line) and  $a_w = 0.06$  (pink line). The deconvolution in Gaussian components is related to the spectrum of the sample at the higher hydration degree. The main components band are as follows:  $\alpha$ -helix at 1338, 1320 and 1300  $\text{cm}^{-1}$ ,  $\beta$  sheet at 1230  $\text{cm}^{-1}$  and unordered structures at 1260  $\text{cm}^{-1}$  and 1285  $\text{cm}^{-1}$ .

In **Figure 12**, the percentage amount of each component band corresponding to each secondary structure element was plotted as a function of the increasing water activity  $a_w$  settled in the dry box.

It appears that dehydration treatment induces small but significant conformational changes involving the increase in the  $\beta$  structure fraction. Interestingly, the plot points out as the  $\alpha$ -helix

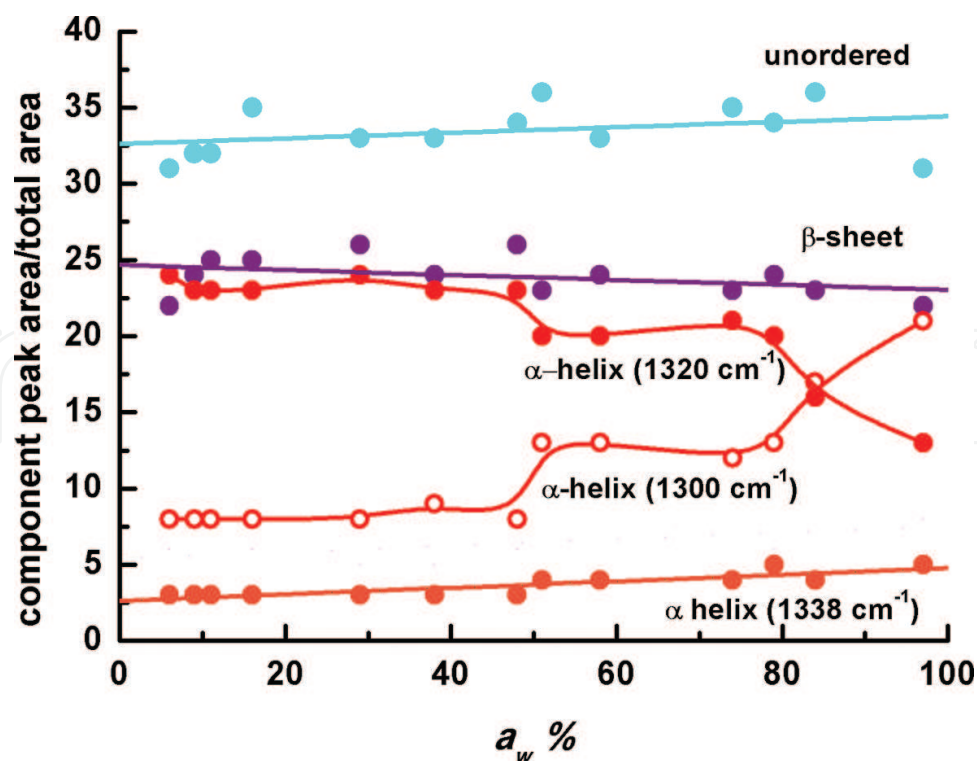


**Figure 12.** Evolution of the amount of secondary structures in lysozyme, monitored by the deconvolution of Amide III band, along the dehydration treatment, plotted as the relative area peak  $A_i/A_{\text{tot}}$  as a function of the activity  $a_w$ . The color code is related to component bands in **Figure 11**.



portion of the protein is heavily affected by water subtraction. The two bands peaking at 1320 and 1300  $\text{cm}^{-1}$ , related to this conformational motif, reveal a mutual amplitude interconversion following a stepped trend, similar but specular, as a function of water content changes. The observed effect could be related to small conformational changes, as a result of hydration changes, involving different fractions of  $\alpha$ -helices which could be affected by mutual conformational fluctuations. The observed conformational modification may be due to the change in the orientation of two  $\alpha$  domains monitored by the Amide III component bands. Water deprivation could affect intermolecular distances making different helix structure more or less consistent with hydrogen bond. Although this result could not be considered as definitive proof, however, it is important in the understanding the dynamical equilibrium of protein structure, crucial for many biological processes involving the enzyme.

The different response to hydration change of the different polypeptide regions at different secondary structure may be interpreted on the light of the crystallographic studies revealing relatively rigid and flexible regions in the macromolecule [45]. The interdomain dynamics modulated by water interaction could be related to the mechanisms involving the active-site cleft dynamics of the protein needed for the enzymatic activity, whose onset appears over a threshold hydration level and causing the irreversibility of functionality if a critical dehydration threshold is exceeded [41].

## 6. Concluding remarks

The present study amply demonstrated the sensitivity of FTIR technique in the association of biomacromolecule vibrational frequencies to relatively small conformational changes induced by hydration. The critical dependence of the structural properties on the water content may be related to the shape of isotherm curves obtained for  $\nu(\text{OH})$  component bands and in particular to the isteretic behavior of sub-bands. Water molecules set up very intimate interactions with biological macromolecules. Their structural rearrangement induced by water deprivation would provide local restructuring of the molecule and modification in the exposition of the side chain groups. The first effect, portrayed by  $\nu(\text{OH})$  stretching band, affects the second one, monitored by changes in fingerprint characteristic features. The critical interrelations between the hydration shell and the relative mobility of different regions of the molecule allows considerable progresses in this field accounting for the loss of enzymatic activity and functionality for proteins [41], phase transition in lipid assembly [10] and change in physical properties for melanins [9], in conditions of extreme dehydration.

## Author details

Maria Grazia Bridelli

Address all correspondence to: mariagrazia.bridelli@unipr.it

Department of Physics and Earth Sciences "Macedonio Melloni," University of Parma, Parma, Italy

## References

- [1] Franks F, Water: 2nd Edition. A Matrix of Life. RSC Paperbacks, Cambridge, UK; 2000.
- [2] Gregory R B, editor. Protein–Solvent Interactions. New York: Dekker; 1995.
- [3] Levy Y and Onuchic J N: Water mediation in protein folding and molecular recognition. *Annu. Rev. Biophys. Biomol. Struct.* 2006;35:389–415.
- [4] Rupley J A, Gratton E and Careri G: Water and globular proteins. *Trends Biochem. Sci.* 1983;8:18–22.
- [5] Rupley J A and Careri G: Protein hydration and function. *Adv. Protein Chem.* 1991;41:37–172.
- [6] Raschke T M: Water structure and interactions with protein surfaces, *Curr. Opin. Struct. Biol.* 2006;16:152–159.
- [7] Wernet Ph et al: The structure of the first coordination shell in liquid water, *Science* 2004;304:995–999.
- [8] Mantsch H H, Chapman D. editors. *Infrared Spectroscopy of Biomolecules*. Wiley-Liss, Inc, New York; 1996.
- [9] Bridelli M G, Crippa P R: Infrared and water sorption studies of the hydration structure and mechanism in natural and synthetic melanin. *J. Phys. Chem. B.* 2010;114:9381–9390.
- [10] Bridelli M G, Capelletti R, Mora C: Structural features and functional properties of water in model DMPC membranes: thermally stimulated depolarization currents (TSDCs) and Fourier transform infrared (FTIR) studies. *J. Phys. D: Appl. Phys.* 2013;46:485401
- [11] Falk M and Ford T A: Infrared spectrum and structure of liquid water. *Can. J. Chem.* 1966;44:1699–1707.
- [12] Auer B M, Skinner J L: IR and Raman spectra of liquid water: theory and interpretation. *J. Chem. Phys.* 2008;128:224511.
- [13] Brubach J B et al.: Signatures of the hydrogen bonding in the infrared bands of water. *J. Chem. Phys.* 2001;122:184509.
- [14] Buontempo U, Careri G, Fasella P: Hydration water of globular proteins: the infrared band near 3300 cm<sup>-1</sup>. *Biopolymers* 1972;11:519–521.
- [15] Onori G, Santucci A, IR investigations of water structure in aerosol OT reverse micellar aggregates. *J. Phys. Chem.* 1993;97:5430–5434.
- [16] Mallamace F et al.: Role of the solvent in the dynamical transitions of proteins: the case of the lysozyme-water system. *J. Chem. Phys.* 2007;127:045104.
- [17] Schmidt D A and Miki K: Structural correlations in liquid water: a new interpretation of IR spectroscopy. *J. Phys. Chem. A.* 2007;111:10119–10122.

- [18] Badger R M: A relation between internuclear distances and bond force constants. *Chem. J. Phys.* 1934;2:128–131.
- [19] Bridelli M G, Capelletti R, Maraia F, Mora C, Pirola L: Initial hydration steps in lipase studied by means of water sorption isotherms, FTIR spectroscopy and thermally stimulated depolarization currents. *J. Phys. D: Appl. Phys.* 2002;35:1039–1048.
- [20] Atkins P and de Paula J, *Physical Chemistry*. 7th Edition. Oxford University Press, Oxford, UK; 2002.
- [21] Byler D M and Susi H: Examination of the secondary structure of proteins by deconvolved FTIR spectra. *Biopolymers*. 1986;25:469–487.
- [22] Gregg S J, Sing K S W, *Adsorption, Surface Area, and Porosity*. Academic Press: New York; 1982.
- [23] Nakamoto K, Margoshes M, Rundle RE: Stretching frequencies as a function of distances in hydrogen bonds. *J. Am. Chem. Soc.* 1955;77:6480–6486.
- [24] Venyaminov S Yu, Prendergast F G: Water (H<sub>2</sub>O and D<sub>2</sub>O) molar absorptivity in the 1000–4000 cm<sup>-1</sup> range and quantitative infrared spectroscopy of aqueous solutions. *Anal. Biochem.* 1997;248:234.
- [25] Perumal S, Antipova O, Orgel J P R O: Collagen fibril architecture, domain organization, and triple-helical conformation govern its proteolysis. *Proc. Natl. Acad. Sci. U S A* 2008;105(8):2824–2829.
- [26] Shoulders M D, Raines R T: Collagen structure and stability. *Annu. Rev. Biochem.* 2009;78:929–958.
- [27] Kotch F W, Raines R T P: Self-assembly of synthetic collagen triple helices. *Proc. Natl. Acad. Sci. U S A*. 2006;103(9):3028–3033.
- [28] Kawahara K, Nishi Y, Nakamura S, Uchiyama S, Nishiuchi Y, Nakazawa T, Ohkubo T, and Kobayashi Y: Effect of hydration on the stability of the collagen-like triple-helical structure of [4(R)-Hydroxyprolyl-4(R)-hydroxyprolylglycine]. *Biochemistry*. 2005;44:15812–15822.
- [29] Bella J, Brodsky B and Berman H M: Hydration structure of a collagen peptide. *Structure*. 1995;3:893–906.
- [30] Bailey A J, Sims T J, Avery N C, Halligan E P: Non-enzymic glycation of fibrous collagen: reaction products of glucose and ribose. *Biochem. J.* 1995;305(Pt 2):385–390.
- [31] Bailey A J, Paul R G, Knott L: Mechanisms of maturation and ageing of collagen. *Mech. Ageing Develop.* 1998;106:1–56.
- [32] Bai P, Phua K, Hardt T, Cernadas M, and Brodsky B: Glycation alters collagen fibril organization. *Connect. Tissue Res.* 1992;28:1–12.
- [33] Hoeve C A J and Tata A S: The structure of water absorbed in collagen. *J. Phys. Chem.* 1978;82:1660–1663.

- [34] Ben-Naim A. Molecular Theory of water and aqueous solutions. Part I: Understanding water. World Scientific Publishing Co. Pte. Ltd., Singapore; 2010.
- [35] Cameron I L, Lanctot A C and Fullerton G D: The molecular stoichiometric hydration model (SHM) as applied to tendon/collagen, globular proteins and cells. *Cell. Biol. Int.* 2011;35:1205–1215.
- [36] Rath A, Davidson A R, Deber C M: The Structure of “Unstructured” Regions in peptides and proteins: role of the polyproline II Helix in protein folding and recognition. *Biopolymers (Peptide Science)*. 2005;80:179–185.
- [37] Matthews B W. In *The Proteins*, Neurath H & Hill R L, editors. 3rd Edition. Vol. 3: 403–590; Academic Press, New York: 1977.
- [38] Kocherbitov V, Arnebrant, and Söderman O: Lysozyme-water interactions studied by sorption calorimetry. *J. Phys. Chem. B.* 2004;108(49):19036–19042.
- [39] Shah N K and Ludescher R: Influence of hydration on the internal dynamics of hen egg white lysozyme in the dry state. *Photochem. Photobiol.* 1993;58(2):169–174.
- [40] Bridelli M G, Capelletti R, and Vecli A: Sequential hydration-dehydration studies of lysozyme by the thermally stimulated depolarization currents (TSDC) technique. *J. Biochem. Biophys. Methods.* 1992;24:135–146.
- [41] Careri G, Gratton E, Yang P H and Rupley J A: Correlation of IR spectroscopic, heat capacity, diamagnetic susceptibility and enzymatic measurements on lysozyme powder. *Nature.* 1980;284:572–573.
- [42] Barth A and Zscherp C: What vibrations tell us about proteins. *Q. Rev. Biophys.* 2002;35(4):369–430.
- [43] Bridelli M G, Capelletti R: Hydration structure analysis of lysozyme amyloid fibrils by thermally stimulated depolarization currents (TSDC) technique. *Spectroscopy.* 2008;22:165–176.
- [44] Bramanti E, Benedetti E: Determination of the secondary structure of isomeric forms of serum Albumin by a particular frequency deconvolution procedure applied to Fourier transform analysis. *Biopolymers.* 1996;38:639–653.
- [45] Madhusudan, and Vijayan M: Rigid and flexible region in lysozyme and the invariant features in its hydration shell. *Current Science (Bangalore)* 1991;60(3):165–170.

